Cell Death and Differentiation (2009) 16, 858–868

www.nature.com/cdd

Abrogation of DNA vector-based RNAi during apoptosis in mammalian cells due to caspase-mediated cleavage and inactivation of Dicer-1

MM Ghodgaonkar[1,4], RG Shah[1], F Kandan-Kulangara[1], E-B Affar[2,5], HH Qi[2], E Wiemer[3] and GM Shah*[,1]

RNA interference (RNAi) is used as a reverse-genetic tool to examine functions of a gene in different cellular processes including apoptosis. As key cellular proteins are inactivated during apoptosis, and as RNAi requires cooperation of many cellular proteins, we examined whether DNA vector-based RNAi would continue to function during apoptosis. The short hairpin RNA transcribed from the DNA vector is processed by Dicer-1 to form small interfering RNA that is incorporated in the RNA-induced silencing complex (RISC) to guide a sequence-specific silencing of the target mRNA. We report here that DNA vector-based RNAi of three different genes, namely poly(ADP-ribose) polymerase-1, p14^{ARF} and lamin A/C are abrogated during apoptosis. The failure of DNA vector-based RNAi was not at the level of Ago-2 or RISC-mediated step of RNAi but due to catalytic inactivation of Dicer-1 on specific cleavage at the STTD^{1476} and CGVD^{1538} sites within its RNase IIIa domain. Using multiple approaches, caspase-3 was identified as the major caspase responsible for the cleavage and inactivation of Dicer-1. As Dicer-1 is also the common endonuclease required for formation of microRNA (miRNA) in mammalian cells, we observed decreased levels of mature forms of miR-16, miR-21 and let-7a. Our results suggest a role for apoptotic cleavage and inactivation of Dicer-1 in controlling apoptotic events through altered availability of miRNA.
Cell Death and Differentiation (2009) **16,** 858–868; doi:10.1038/cdd.2009.15; published online 20 February 2009

RNA interference (RNAi) including the microRNA (miRNA) pathway is an evolutionarily conserved mechanism for sequence-specific gene silencing by small (21–26 nucleotides) guide RNA.[1,2] There are two main types of RNAi-inducing small guide RNA: the endogenously generated miRNA, which are derived from long stem-loop structured precursors, and small interfering RNA (siRNA), which may be either exogenously supplied as short or long dsRNA or produced in the cells from a DNA vector-directed short hairpin RNA (shRNA).[2] Regardless of the origin of the small regulatory RNA, the key steps responsible for achieving RNAi are essentially the same and require controlled and coordinated participation of the host–cell machinery. Briefly, different types of precursor RNA, such as the long dsRNA, shRNA transcribed from a DNA vector or pre-processed hairpin pre-miRNA, are first converted to small regulatory RNA by the endoribonuclease Dicer-1 in the cytoplasm of mammalian cells. These are then loaded into the RNA effector complexes known as RNA-induced silencing complex (RISC) to guide the machinery to the target mRNA in a sequence-specific manner. Depending on the extent of sequence homology, gene silencing is achieved by cleavage or destabilization of the target cognate mRNA or by inhibition of its translation.[3]

RNAi is increasingly being explored to characterize the roles of miRNA in regulating apoptosis.[3,4] In addition, shRNA-based RNAi is also being exploited for understanding the role of a given gene in apoptosis.[5–7] However, as many key cellular proteins are cleaved by caspases during apoptosis,[8] it is pertinent to examine whether apoptotic events compromise the integrity of the core machinery of the RNAi pathway. A recent study reporting specific stimuli-dependent cleavage of Dicer-1 during apoptosis,[9] further warrants a need for characterization of the impact of apoptosis on DNA vector-based RNAi, a process which requires full functionality of Dicer-1-dependent formation of the siRNA from the precursor shRNA and the RISC-dependent silencing of the target mRNA. We used the DNA vector-based RNAi model for three different genes: namely poly(ADP-ribose) polymerase-1 (PARP),[10] a model that has allowed us to reveal its novel functions in the nucleotide excision repair of UV-damaged DNA,[11] inactivation of X chromosome[12] and in growth or chemosensitivity of melanoma cells;[13] the tumor suppressor gene p14^{ARF} and the nuclear protein lamin A/C. We report

[1]Laboratory for Skin Cancer Research, Faculty of Medicine, CHUL Research Center (CHUQ), Laval University, Quebec, QC, Canada G1V 4G2; [2]Department of Pathology, Harvard Medical School, Boston, MA 02115, USA and [3]Department of Medical Oncology, Erasmus Medical Center, Josephine Nefkens Institute, 3000 CA, Rotterdam, The Netherlands
*Corresponding author: GM Shah, Laboratory for Skin Cancer Research, CHUL Hospital Research Centre of Laval University, Door B-0016, 2705, Laurier Boulevard, Quebec, QC, Canada G1V 4G2. Tel: +418 656 4141/Ext. 48259; Fax: +418 654 2739; E-mail: girish.shah@crchul.ulaval.ca
[4]Current address: Institute of Molecular Cancer Research, Zurich, Switzerland.
[5]Current address: Maisoneuve Rosemont Hospital Research Center, Faculty of Medicine, University of Montreal, Montreal (QC), Canada.
Keywords: apoptosis; RNAi; shRNA; Dicer-1; caspases
Abbreviations: RNAi, RNA interference; RISC, RNA-induced silencing complex; siRNA, small interfering RNA; miRNA, microRNA; PARP, poly(ADP-ribose) polymerase-1
Received 31.7.08; revised 15.1.09; accepted 19.1.09; Edited by G Salvesen; published online 20.2.09

here that the DNA vector-based RNAi of all three genes is abrogated during apoptosis. We extensively characterized the failure of RNAi and identified its cause to be a specific dual cleavage and catalytic inactivation of Dicer-1. We used multiple approaches to show that caspase-3 is the major caspase responsible for this cleavage and inactivation of Dicer-1. We also show that Dicer-1 cleavage during apoptosis is associated with decreased formation of some of the mature miRNA, suggesting a larger role of Dicer-1 cleavage in control of apoptosis.

Results

Abrogation of DNA vector-based RNAi of PARP during apoptosis. The effect of apoptotic events on the efficacy of DNA vector-based RNAi was examined first in our earlier reported[10] PARP-replete (GMU6) or PARP-depleted (GMSiP) human skin fibroblasts (Figure 1a). The induction of apoptosis by treatment with different agents was accompanied by cleavage/activation of caspase-3 to its large subunit at 17/19 kDa, and cleavage of PARP to its apoptosis signature 89-kDa fragment in GMU6 cells (Figure 1a, lanes 1–4). The GMSiP cells, which were devoid of PARP before apoptosis, surprisingly, displayed 89-kDa PARP fragment during apoptosis (Figure 1a, lanes 5–8). The probing with an 89-kDa PARP fragment-specific antibody confirmed that this major band in apoptotic GMSiP cells co-migrated with the band in the apoptotic HL-60 or GMU6 cells (Figure 1b and Supplementary Figure S1a).

For an 89-kDa PARP fragment to appear in PARP-depleted GMSiP cells, full-length PARP has to be made, which suggests that PARP-mRNA must no longer be subjected to degradation by RNAi. This was verified by analyzing the abundance of PARP transcripts by RT-PCR (Figure 1c). The signal for PARP-mRNA remained almost unchanged in UVB-treated GMU6 cells, but it went from undetectable amounts at 0 h to a significant increase at 48 h in UVB-treated GMSiP cells. The reappearance of mRNA and the presence of caspase-cleaved 89-kDa PARP fragment confirmed that DNA vector-based RNAi of PARP was abrogated in the apoptotic GMSiP cells.

The fact that apoptosis-associated failure of DNA vector-based RNAi of PARP was not specific for GM-model was confirmed in PARP-depleted CHO-SiP cells[10] (Figure 1d). Different apoptosis-inducing treatments resulted in a dose-dependent increase in activated caspase-3 in both the PARP-phenotypes and cleavage of PARP to its 89-kDa fragment in PARP-replete CHO-U6 cells (Figure 1d, PARP lanes 2–5). However, emergence of the 89-kDa fragment of PARP in the PARP-depleted CHO-SiP cells during apoptosis (Figure 1d, PARP lanes 7–10) confirmed a general nature of apoptosis-associated failure of DNA vector-based RNAi of PARP in mammalian cells.

Failure of DNA vector-based RNAi of $p14^{ARF}$ and lamin during apoptosis. We next examined whether apoptosis-associated abrogation of DNA vector-based RNAi would also occur for two other genes, namely human tumor suppressor gene $p14^{ARF}$ and lamin A/C (Figure 2a and b and Supplementary Figure S1b and c). We generated stable CHO-ARF clone, which expressed HA-tagged human $p14^{ARF}$ and corresponding stable CHO-ARF-shARF clone in which HA-ARF was significantly knocked down by DNA vector-based RNAi (Figure 2a, HA lanes 1, 2 and 6). Induction of apoptosis in CHO-ARF cells by different agents resulted in the formation of activated caspase-3 accompanied by a significant increase in HA-ARF (Figure 2a, HA lanes 3–5), which could be reflecting a transcriptional upregulation similar to that reported for its mouse homolog $p19^{ARF}$ during apoptosis.[14] Interestingly, in the apoptotic shARF cells, there was a robust reappearance of the HA-ARF along with activation of caspase-3 (Figure 2a, lanes 7–9), which clearly indicated failure of DNA vector-based RNAi permitting formation of full length of HA-$p14^{ARF}$.

The lamins A/C, two alternately spliced $\sim$70-kDa proteins arising from a single gene locus, are cleaved by caspase-3-activated caspase-6 to liberate 45- and 28-kDa fragments.[15] Using DNA vector-based RNAi, we generated a HeLa derived shLamin clone with $\sim$75% lamin knockdown (Figure 2b, lamin lanes 1 and 5). Induction of apoptosis in both the lamin phenotypes by various agents was associated with activation of caspase-3 and cleavage of PARP to its 89-kDa fragment (Figure 2b, caspase-3 and PARP panels). Lamins A/C were also cleaved to their $\sim$28-kDa Δlamin fragment in the apoptotic HeLa cells with a ratio of 0.2–0.5 for Δlamin/intact lamins. In contrast, there was a much stronger presence of Δlamin fragment during apoptosis in the shLamin cells, which was evident from higher (4.3 and 0.9) ratio of Δlamin/intact lamins during stronger apoptosis-inducing treatments with UVB or staurosporin (Figure 2b, lamin panel). A significantly larger presence of Δlamin indicated that more lamins were being formed and degraded in apoptotic shLamin cells. The apoptosis-associated abrogation of DNA vector-based RNAi of three different genes in different models of apoptosis indicates a universal nature of this observation.

No impact of apoptosis on RISC-dependent RNAi by 21mer siRNA. The abrogation of DNA vector-based RNAi could be caused by failure of one or both the key steps of RNAi, namely Dicer-1-mediated formation of 21mer siRNA from DNA vector-derived shRNA or the RISC-mediated inactivation of the target mRNA. To distinguish between these two steps, we examined the impact of apoptosis on RISC-dependent and Dicer-independent transient RNAi by 21mer siRNA of GFP and PARP (Figure 2c). A high level of GFP expression achieved in the GFP cDNA-transfected human skin fibroblasts GM637 was significantly suppressed by co-transfection with GFP-targeting 21mer siRNA (Figure 2c, GFP lanes 2, 4 and 6). Induction of apoptosis by etoposide resulted in a strong caspase-3 activation, but it was not accompanied by any change in the status of GFP-knockdown (Figure 2c, lanes 6–7). Similarly, a significant PARP-knockdown achieved by its corresponding 21mer siRNA was not abrogated during etoposide-induced apoptosis, because the signal for its 89-kDa fragment seemed to be mainly due to partial digestion of the residual PARP in these cells after knockdown (Figure 2c, lanes 10–11). Thus, unlike the SiP model in which the emergence of the 89-kDa PARP-fragment during apoptosis was due to

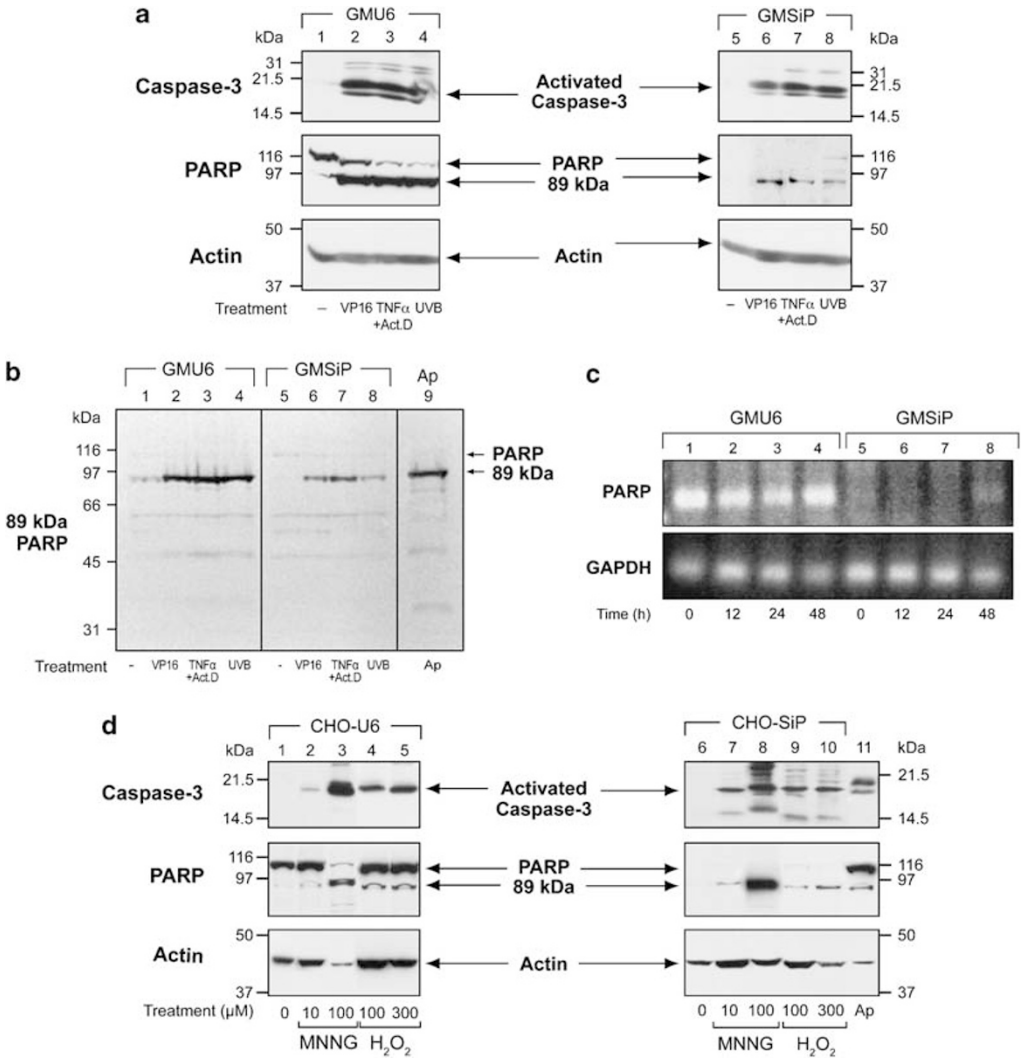

Figure 1 Abrogation of DNA vector-based RNAi of PARP during apoptosis. (**a**) Failure of RNAi of PARP in GMSiP cells. In the stable PARP-replete GMU6 and PARP-depleted GMSiP human skin fibroblasts, apoptosis was induced by treatment with 100 μM VP-16 for 18 h, 1200 U/ml TNFα + 0.25 μg/ml actinomycin D for 18 h or 1600 J/m^2 UVB for 48 h. Whole cell extracts were immunoblotted with cleaved/activated caspase-3 antibody that detects the larger 19/17-kDa fragment of caspase-3 and with a monoclonal antibody to PARP that detects both the full-length PARP and its 89-kDa apoptotic fragment. Actin immunoprobing served as loading control and results shown here represent similar results obtained with at least five independent experiments. (**b**) Identification of 89-kDa PARP fragment in apoptotic GMSiP cells. The cell extracts from GMU6 and GMSiP cells treated with apoptosis-inducing treatments as described above were probed with antibody specific for the 89-kDa apoptotic fragment of PARP. The Ap lane refers to extract from apoptotic HL-60 cells treated with 70 μM etoposide for 8 h. The ponceau-S staining of the blot served as loading control (see Supplementary Figure S1a). The results shown here represent similar results obtained with three independent experiments. (**c**) Emergence of PARP-mRNA in apoptotic GMSiP cells. GMU6 and GMSiP cells were irradiated with 1600 J/m^2 UVB and at indicated time points; RNA was extracted and analyzed by RT-PCR. Upper panels indicate the levels of PARP-mRNA, whereas lower panel indicates the levels of GAPDH-mRNA, which was used as a control. The results shown here represent similar results obtained with two independent experiments. (**d**) Failure of PARP-RNAi in CHO-SiP cells. PARP-replete CHO-U6 and PARP-depleted CHO-SiP cells were treated with two doses of MNNG or H_2O_2 for 24 h and immunoblotted for caspase-3 and PARP. Actin was probed as loading control and Ap refers to apoptotic HL-60 cells, as described above for panel **b**. The results shown here represent similar results obtained with three independent experiments

the failure of stable shRNA, the feeble appearance of the 89-kDa PARP fragment in the transient knockdown model was not due to the failure of 21mer siRNA during apoptosis. Although one could not exclude subtle differences in the influence of apoptotic events on the transient knockdown of an exogenous gene GFP *versus* an endogenous gene PARP, our collective results revealed a general lack of effect of apoptosis on RISC-dependent RNAi by 21mer siRNA. Thus, abrogation of DNA vector-based RNAi must be due to failure of events upstream of the RISC step.

Selective cleavage of endonuclease Dicer-1 during apoptosis. The caspases strategically cleave a selected number of proteins to facilitate apoptosis,[8] hence we examined integrity of the principal RNases implicated in the two key steps of DNA vector-based RNAi in mammalian cells, namely Dicer-1 and RISC-member Ago-2.[16] In two of the human cell line models described above (GMSiP and HeLa-shLamin), apoptosis had no effect on the integrity of Ago-2, whereas the 230-kDa Dicer-1 was cleaved to a $\sim$180-kDa ΔDicer-1 fragment (Figure 3a and b). Owing to

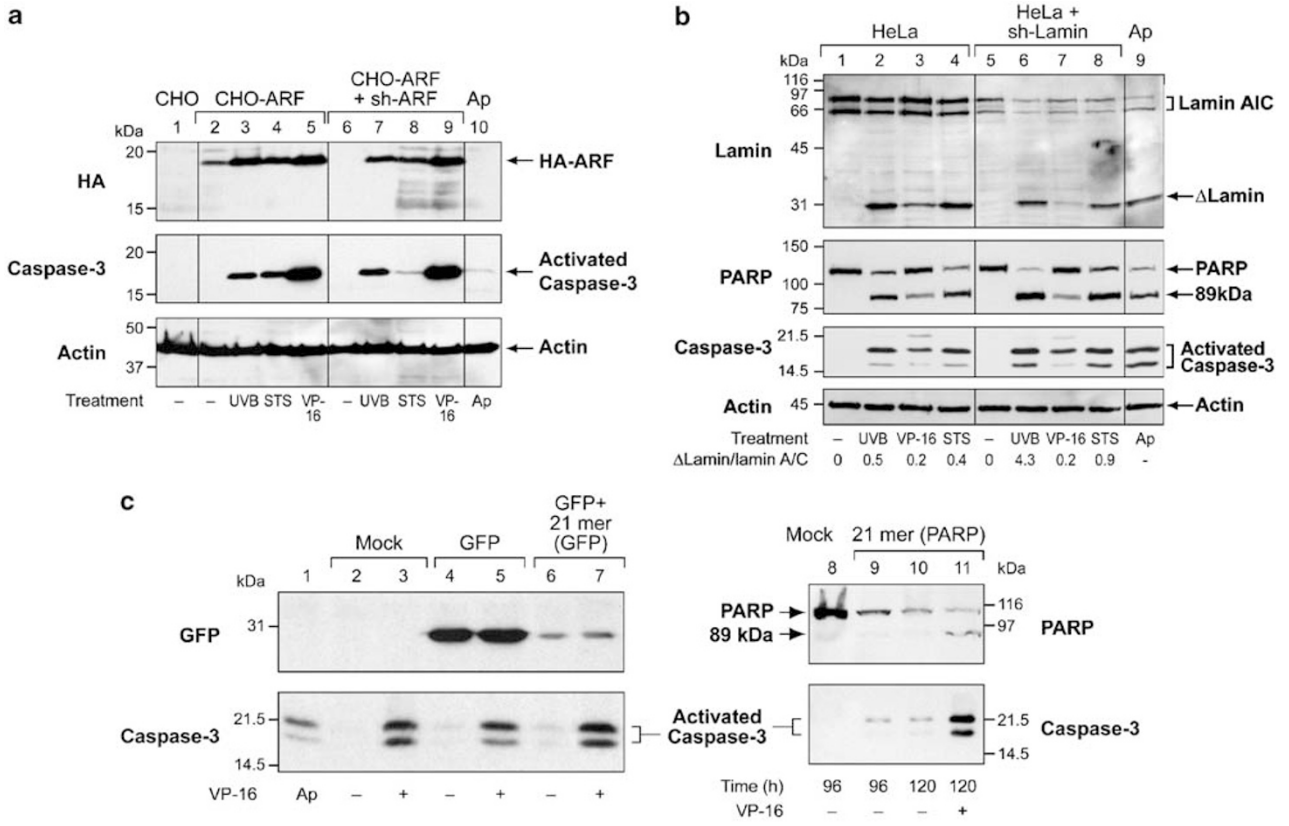

Figure 2 Apoptosis-associated failure of stable shRNA of $p14^{ARF}$ and lamin, but not that of transient RNAi of GFP and PARP by 21mer siRNA. (**a**) Failure of shRNA of HA-$p14^{ARF}$. The CHO-ARF clone expressing HA-tagged human $p14^{ARF}$ or CHO-ARF-shARF clone in which the HA-ARF expression was knocked down by DNA vector-based RNAi were treated with 1600 J/m^2 UVB for 32 h, 1 μM staurosporin for 18 h or 100 μM etoposide (VP-16) for 32 h. The cell extracts were immunoblotted for HA and activated caspase-3. Actin immunoprobing served as loading controls and Ponceau-S membrane staining is shown in Supplementary Figure S1b. The results shown here represent similar results obtained with three independent experiments. (**b**) Failure of shRNA of lamin in HeLa–shLamin cells. The lamin-replete HeLa cells and lamin-depleted HeLa–shLamin cells were treated with three apoptosis-inducing treatments, as described above for shARF panel. The immunoprobing was carried out for lamin, activated caspase-3 and PARP. The ratio of ΔLamin/lamins A/C was derived from densitometric measurement of the signals for these bands. Actin immunoprobing served as loading controls and Ponceau-S membrane staining is shown in Supplementary Figure S1c. The results shown here represent similar results obtained with three independent experiments. (**c**) Lack of failure of transient RNAi of GFP and PARP by 21mer siRNA during apoptosis. GM637 cells were transiently transfected with cDNA of GFP ± GFP-targeting 21mer dsRNA for 48 h (left panel) or with pcDNA I/neo ± PARP-targeting 21mer dsRNA (right panel) for 96 h followed by treatment with 100 μM etoposide (VP-16) for 18 or 24 h, respectively. The cell extracts were immunoblotted for activated caspase-3 and GFP or PARP. The results shown here represent similar results obtained with at least three independent experiments

lack of specific antibody, we could not confirm Dicer-1 cleavage in hamster (CHO) model, but we reasoned that this cleavage must be a general phenomenon observable in any model of apoptosis. Hence, we examined integrity of Ago-2 and Dicer-1 in two of the well-established models of apoptosis, that is, HL-60 (Figure 3c) or HeLa (Figure 3d) cells. The time course of apoptosis in response to treatment with diverse agents revealed that once caspase-3 was activated, PARP was cleaved to its 89-kDa apoptotic fragment. In these models, Ago-2 remained intact, whereas Dicer-1 was cleaved to its 180-kDa fragment (Figure 3c and d), confirming the universal nature of Dicer-1 cleavage to a 180-kDa fragment during apoptosis in human-derived cells.

Identification of caspase responsible for cleavage of Dicer-1 during apoptosis. To examine if any of the caspases were responsible for cleavage of Dicer-1 during apoptosis, we used three independent approaches, namely broad-spectrum caspase inhibitor, *in vitro* caspase assays and a caspase-deficient cell line. The broad-spectrum caspase inhibitor zVAD-fmk could efficiently suppress caspase-3 activation and cleavage of Dicer-1 during staurosporin-induced apoptosis in COS-1 cells (Figure 4a).

To identify the specific caspase responsible for Dicer-1 cleavage, an immunopurified N-terminal FLAG-tagged Dicer-1 was cleaved by caspases-1 to 10 *in vitro* (Figure 4b). As a positive control for the *in vitro* caspase assay, we confirmed that caspases-3 and -7 could cleave PARP to its signature 89-kDa fragment[17] (Figure 4b, top panel). The caspase-cleavage products of N-terminal FLAG-tagged hDicer-1 were identified by probing with anti-Dicer 1 antibody that recognizes an epitope in the N-terminal half of the protein and the anti-FLAG antibody that detects N-terminal FLAG (Figure 4b). The probing with anti-Dicer-1 antibody revealed that almost all caspases, notably 1, 3, 5 and 7, could generate some amount of ~180-kDa Dicer-1 fragment (Figure 4b: Dicer-1 panel). The FLAG probing, however, revealed that only caspases-3, -5 and -7 generated

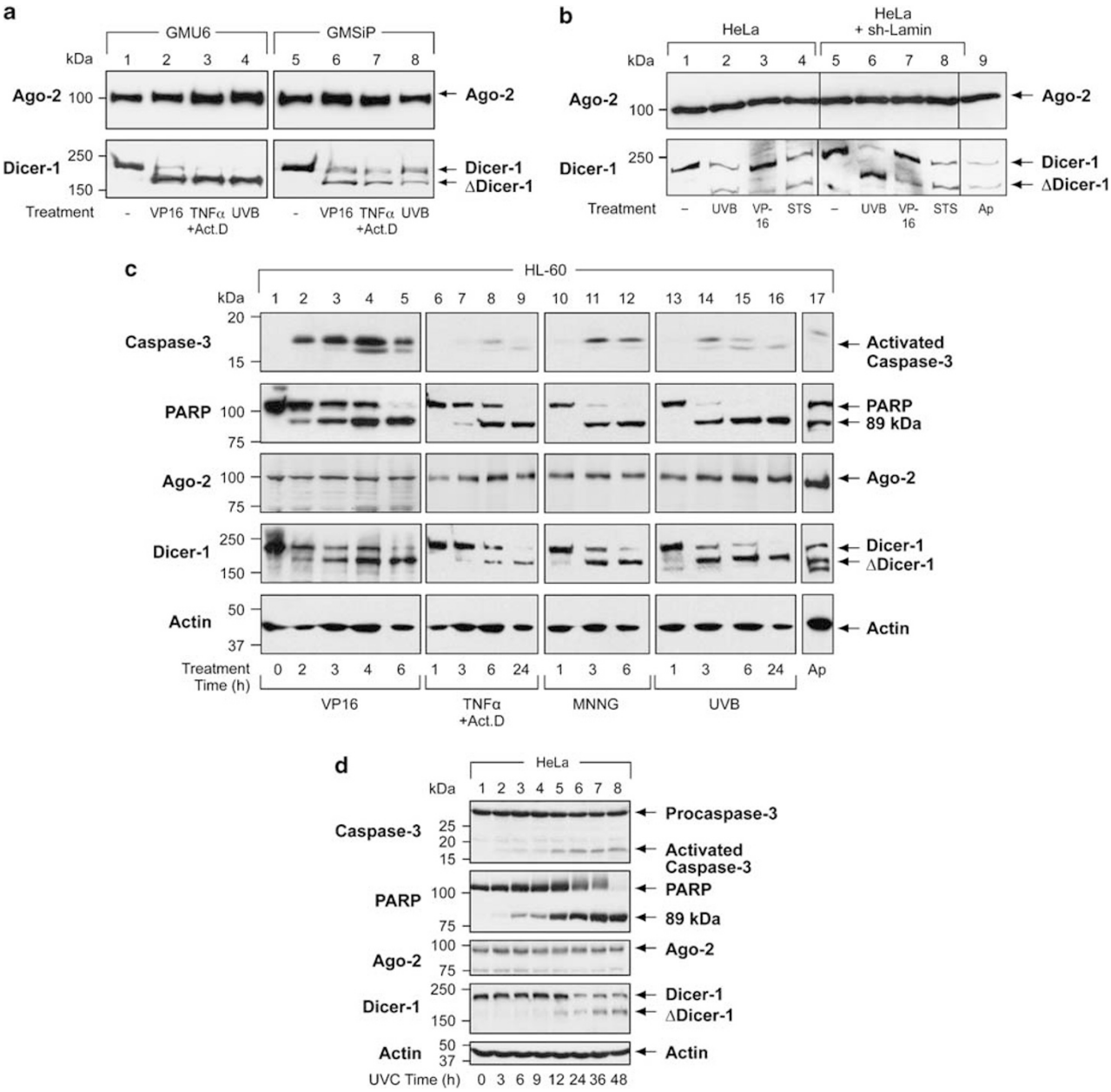

Figure 3 Cleavage of Dicer-1 in human cell lines undergoing apoptosis. (**a**) GMU6 and GMSiP; (**b**) HeLa and HeLa–shLamin; (**c**) HL-60 and (**d**) HeLa were treated with different apoptosis-inducing conditions. The GMU6/GMSiP and HeLa/HeLa-shLamin cells were treated with etoposide (VP-16), TNFα + actinomycin D, staurosporin or UVB as specified in Figures 1a and 2b. The HL-60 cells were treated with the three conditions as above, as well as 100 μM MNNG for the specified time. HeLa cells were treated with 10 J/m^2 UVC and harvested at specified time. The cell extracts were subjected to immunoblotting for activated caspase-3, PARP, Ago-2 and Dicer-1. Cleaved proteins are indicated as 89 kDa (for cleaved PARP) and ΔDicer-1 (for cleaved Dicer-1). Actin probing served as loading controls for panels **c** and **d**, whereas loading control for samples in panels **a** and **b** were shown in Figures 1a and 2b. Results shown in all three panels represent similar results obtained with at least two to three independent experiments. Ap lane in panels **b** and **c** refers to 70 μM etoposide (VP-16, 8 h)-treated apoptotic HL-60 cells

major FLAG-positive bands at about 180, 150 and 130 kDa, respectively (Figure 4b: FLAG panel). Thus, only caspase-3 cleavage resulted in a major 180-kDa Dicer-1 fragment with an intact N-terminal FLAG, whereas other caspases had additional cleavages at the N- or C-termini.

To identify which of these cleavage patterns *in vitro* reflected cellular cleavage of Dicer-1, we examined apoptotic cleavage of hDicer-1 tagged with N-terminal FLAG and C-terminal HA after its expression in COS-1 cells (Figure 4c). The intact hDicer-1, detectable by both FLAG and HA antibodies in the untreated cells, was degraded to a FLAG-positive 180-kDa and HA-positive major $\sim$42-kDa and minor $\sim$50-kDa fragments during apoptosis (Figure 4c, lanes 2 and 4). The formation of a FLAG-positive 180-kDa ΔDicer-1 fragment with an intact N-terminus in apoptotic cells was consistent with caspase-3 digestion of Dicer-1 *in vitro*.

Finally, we examined if Dicer-1 would be cleaved during apoptosis in caspase-3-deficient[18] MCF-7 cells (Figure 4d).

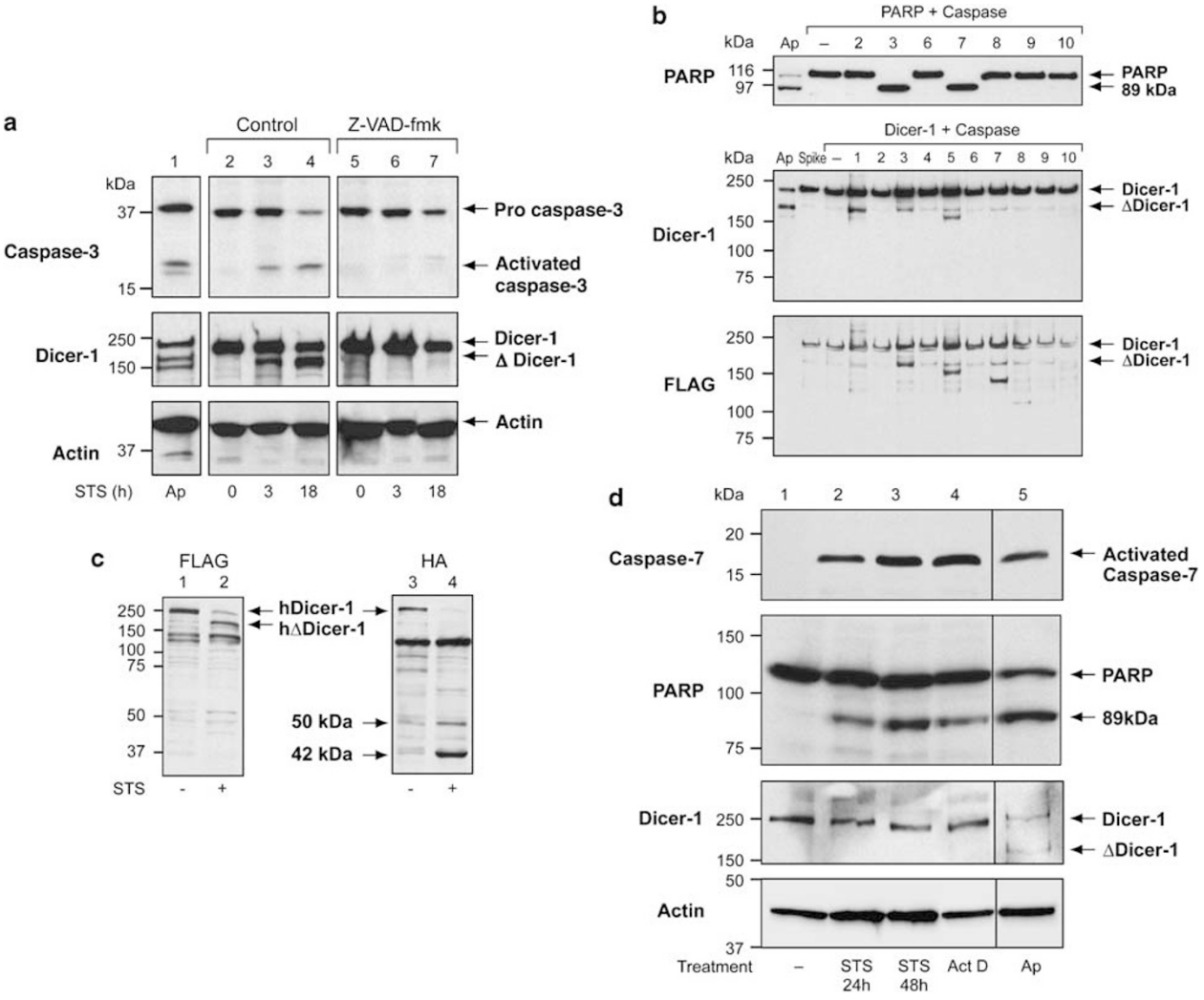

Figure 4 Identification of caspase responsible for cleavage of Dicer-1. (**a**) Caspase-inhibitor zVAD-fmk blocks cleavage of Dicer-1. COS-1 cells were incubated with 50 μM zVAD-fmk (Calbiochem) at 37°C for 90 min before treatment with 1 μM staurosporin (STS) for specified time. The samples were harvested and immunoblotted for activated caspase-3 and Dicer-1. Ap lane refers to 70 μM etoposide (VP-16, 8 h)-treated apoptotic HL-60 cells. Actin immunoprobing served as loading control and results shown here represent similar results obtained with two independent experiments. (**b**) *In vitro* cleavage of recombinant hDicer-1 by various caspases. The immunopurified and eluted FLAG-hDicer-1 was digested with ten different recombinant caspases (1–10) in an *in vitro* caspase digestion assay. The samples were probed by western blotting for Dicer-1 or FLAG. Ap refers to apoptotic HL-60 cell extract (described in panel **a**), which served as a positive control for full-length Dicer-1 and its cleaved fragment ΔDicer-1. (**c**) Identification of apoptotic fragments of FLAG-hDicer-1-HA in apoptotic cells. COS-1 cells transfected with FLAG-hDicer-1-HA cDNA were treated after 48 h with 1 μM staurosporin (STS) for 18 h to induce apoptosis. Whole cell extracts prepared from the control or apoptotic cells were immunoblotted for FLAG or HA to identify the intact protein or N-terminal FLAG-bound or C-terminal HA-bound fragments. The results shown here represent similar results obtained with four independent experiments. (**d**) Lack of Dicer-1 cleavage in caspase-3-deficient MCF-7 cells during apoptosis. MCF-7 cells were treated with 5 μM staurosporin or 5 μg/ml actinomycin D for 48 h; and immunoblotted for activated caspase-7, PARP and Dicer-1. Ap refers to apoptotic HL-60 cell extract (described in panel **a**). Actin immunoprobing served as loading control and results shown here represent similar results obtained with three independent experiments

During staurosporin or actinomycin-induced apoptosis, there was a caspase-7 activation and cleavage of PARP to its 89-kDa fragment, but Dicer-1 was not cleaved to its 180-kDa fragment. Collectively, these results indicated that caspase-3 is the major, if not the only, caspase responsible for cleavage of Dicer-1 to its 180-kDa N-terminal fragment during cellular apoptosis.

Identification of apoptotic cleavage sites in Dicer-1. To identify the apoptotic cleavage sites of FLAG-hDicer-1-HA, the N-terminal 180-kDa and C-terminal 42-kDa fragments, immunoprecipitated following experimental conditions similar to that in Figure 4c, were subjected to mass spectrometry analyses after tryptic digestion. In the 180-kDa fragment, there was a continuous presence of the tryptic fragments from the N-terminus up to STTD^{1476}, whereas ^{1578}AAQL was the first tryptic fragment in the C-terminal 42-kDa fragment, indicating that cleavage occurred between these two sites in RNase IIIa domain of Dicer-1 (Supplementary Figure S2).

There are at least seven putative caspase-cleavage XXXD motifs[8] in this region in which a cleavage at D could give rise to 42- or 50-kDa C-terminal fragment (Figure 5a). These seven D residues were mutated to A and single mutants were expressed in COS-1 cells, which were subjected to apoptosis.

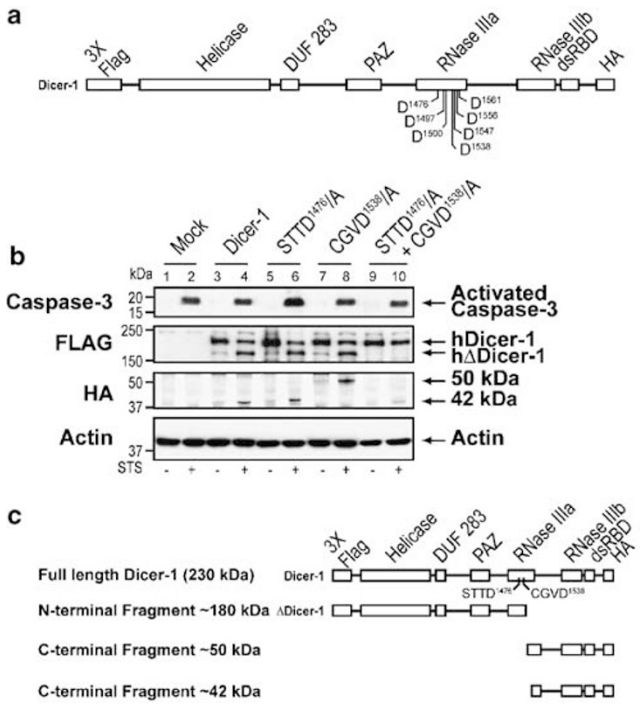

Figure 5 Identification of the cleavage site for Dicer-1. (**a**) The seven putative caspase-target D residues in RNase IIIa domain of hDicer-1. Based on the MS–MS data of apoptotic cleavage fragments of hDicer-1 immunoprecipitated from FLAG-hDicer-1-HA expressing COS-1 cells, seven Asp (D) residues were identified and mutated to caspase-uncleavable D/A. The full Dicer-1 sequence, its functional motifs and D residues of interest are shown in Supplementary Figure S2. (**b**) Identification of the cellular apoptotic cleavage sites in Dicer-1. The cDNA for wild-type Dicer-1, its single mutants $STTD^{1476}$/A and $CGVD^{1538}$/A or its double mutant $STTD^{1476}$/A:$CGVD^{1538}$/A were expressed in COS-1 cells for 48 h prior to treatment with 1 μM staurosporin (STS) for 18 h to induce apoptosis. The samples were immunoblotted for activated caspase-3 and the N-terminal or C-terminal Dicer-1-fragments were identified by immunoblotting for FLAG or HA. Actin immunoprobing served as loading control and results shown here represent similar results obtained with three independent experiments. (**c**) Schematic representation of the full-length hDicer-1 and its apoptotic fragments. The full-length recombinant FLAG-hDicer-1-HA (230 kDa) gets cleaved to the N-terminal 180 kDa FLAG-detectable ΔDicer-1 fragment, and two C-terminal HA antibody-detectable fragments of ~50 and ~42 kDa generated by cleavage at $STTD^{1476}$ and $CGVD^{1538}$ sites, respectively

Five of these D/A mutations could not prevent cleavage of Dicer-1 (data not shown), but mutations at D^{1476} and D^{1538} sites altered the cleavage of hDicer-1 (Figure 5b). The $STTD^{1476}$/A mutant Dicer-1 was cleaved to generate a FLAG-positive ~180-kDa and HA-positive ~42-kDa fragment, whereas $CGVD^{1538}$/A mutant was cleaved to generate FLAG-positive ~180-kDa and HA-positive ~50-kDa fragments on induction of apoptosis and activation of caspase-3 (Figure 5b, lanes 6 and 8). Therefore, we created and expressed in COS-1 cells, a double mutant D^{1476}/A:D^{1538}/A Dicer-1, which turned out to be completely resistant to cleavage during apoptosis generating neither FLAG- nor HA-positive fragments (Figure 5b, lanes 9–10). Thus, hDicer-1 is cleaved in the apoptotic COS-1 cells at $STTD^{1476}$ to release 50-kDa C-terminal and 180-kDa N-terminal ΔDicer-1 fragments; and C-terminal 50-kDa fragment is further cleaved at $CGVD^{1538}$ to release 42-kDa fragment (Figure 5c).

Inactivation of Dicer-1 and decreased miRNA-formation during apoptosis. As both the cleavage sites of Dicer-1 are located in the catalytically important RNase IIIa domain of hDicer-1, we examined its impact on the catalytic function of Dicer-1 in a dicing assay *in vitro* to convert a 27mer substrate dsRNA to its product 21mer dsRNA.[19] Owing to incompatibility of reagents between caspase and dicing assays, these assays were optimized using FLAG antibody-beads-bound Dicer-1, so as to wash away reagents after each assay. Incubating bead-bound Dicer-1 with caspase-3 resulted in formation of a FLAG- and Dicer-1-positive ΔDicer-1, which was also retained on the FLAG-beads (Figure 6a). The bead-bound intact Dicer-1 was enzymatically active as it converted 27mer dsRNA to 21mer dsRNA in the dicing assay (Figure 6b). That caspase-3 digestion decreased catalytic activity of Dicer-1 was evident from its slower capacity to convert 27mer to 21mer dsRNA from 3–6 h, as compared with intact Dicer-1 (Figure 6c, lanes 2–3 and 6–7). The caspase-3-digested Dicer-1 preparation could eventually convert all the 27mer substrate by 16 h due to the residual intact Dicer-1.

Next, we examined dicing activity in the extracts from control or apoptotic GM637 cells, which had either intact or partially cleaved Dicer-1, respectively (Figure 6d, left panel). Whereas the control cell extract efficiently converted 27mer to 21mer dsRNA in 1–3 h, the apoptotic cell extract failed to convert the substrate up to 3 h (Figure 6d, right panel). A more robust inhibition of dicing activity in the apoptotic cell extract, despite the presence of some intact Dicer-1, reflects additional factors that may negatively influence Dicer-1 activity in apoptotic cells, as compared with assays with *in vitro* partially cleaved Dicer-1 (see discussion). Thus, cleavage of Dicer-1 in apoptotic cells or *in vitro* by casapse-3 was associated with its catalytic inactivation, which could explain the failure of DNA vector-based RNAi during apoptosis.

Unlike other organisms, mammalian cells have only one Dicer homolog (Dicer-1) for both the siRNA production and for the conversion of the pre-miRNA into mature miRNA.[16] Hence, we examined whether Dicer-1 cleavage and inactivation would also influence maturation of three apoptosis-related miRNAs, namely pro-apoptotic miR-16 that regulates anti-apoptotic bcl-2 gene,[20] anti-apoptotic miR-21[21,22] and let-7a miRNA that is both pro-[23] and anti-apoptotic[24] (Figure 6e). In the apoptotic HL-60 cells, there was a decline in the levels of these three mature miRNAs from 6–24 h (Figure 6e, left panel). The quantification of signal for miRNA from two independent experiments showed nearly 40–60% decrease in the signal for these miRNAs at 18–24 h (Figure 6e, right panel). Thus, another consequence of Dicer-1 cleavage by caspase-3 during apoptosis was reduced availability of some of the mature miRNA.

Discussion

We report here that stable knockdown by DNA vector-based RNAi is abrogated during apoptosis in mammalian cells. The data obtained with various cell lines, different apoptosis-inducing treatments and failure of RNAi of three different genes, namely PARP, lamin and $p14^{ARF}$, indicate universal

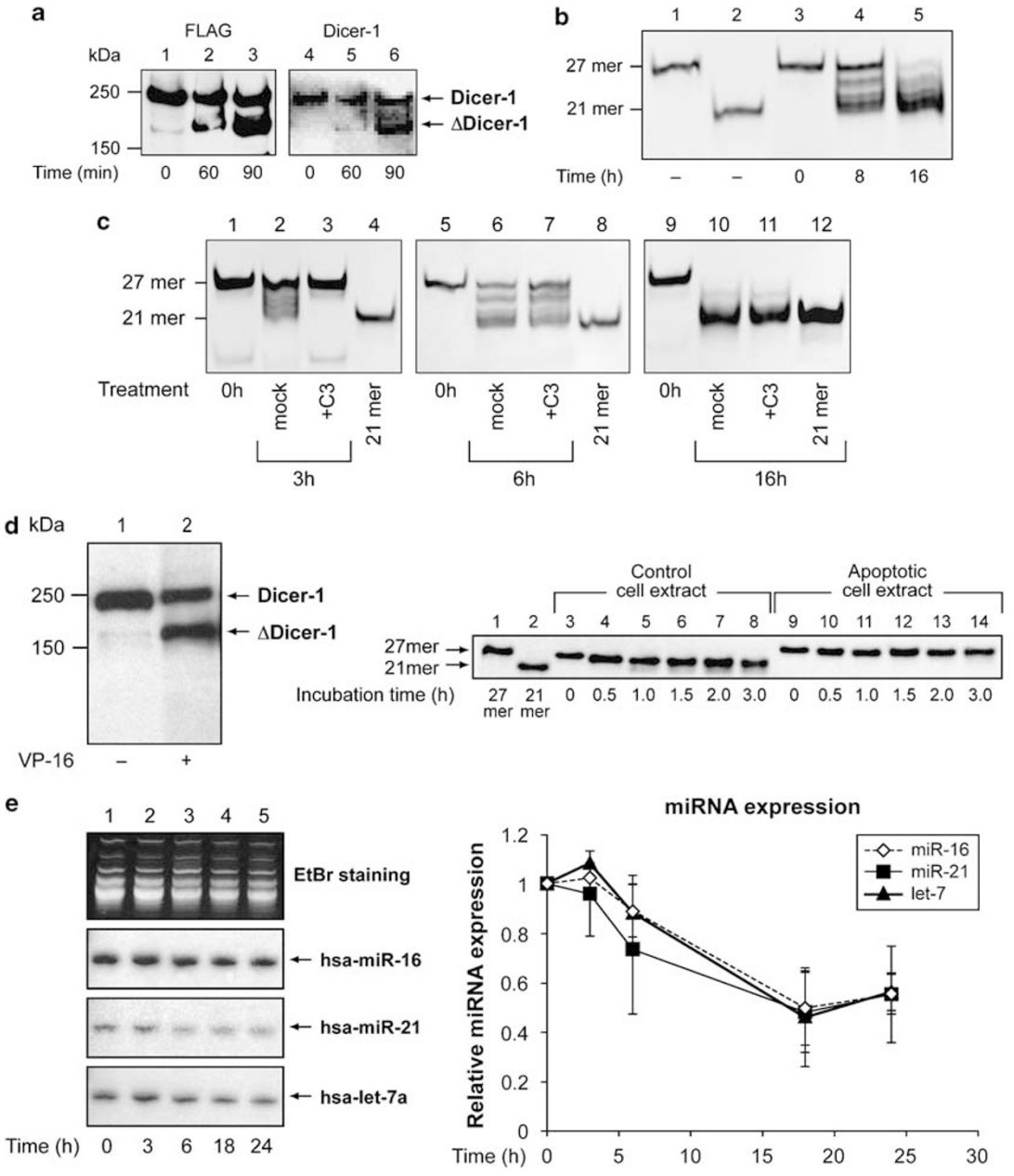

Figure 6 Consequences of cleavage of Dicer-1 during apoptosis: catalytic inactivation and reduced formation of mature miRNA. (**a**) *In vitro* caspase-3-mediated cleavage of immunobead-bound Dicer-1 to its 180-kDa ΔDicer-1 fragment. The immunobead-bound FLAG-hDicer-1 was digested with caspase-3 in an *in vitro* caspase digestion assay. The samples were immunoblotted for FLAG and Dicer-1 to identify intact hDicer-1 and N-terminal 180-kDa ΔDicer-1 fragment. The results shown here represent similar results obtained with three independent experiments. (**b**) *In vitro* catalytic activity of immunobead-bound hDicer-1. The immunobead-bound FLAG-hDicer-1 was incubated with 27mer dsRNA substrate for specified time. The 27mer dsRNA and 21mer dsRNA served as size markers. The samples were resolved on 20% native PAGE and stained with ethidium bromide for visualization of dsRNA bands. The results shown here represent similar results obtained with four independent experiments. (**c**) Catalytic inactivation of hDicer-1 due to caspase-3 digestion. The immunobead-bound FLAG-hDicer-1 was digested with caspase-3 for 90 min followed by catalytic Dicer-1 activity assay, as described above for panels **a** and **b**. The dicing assay samples were harvested at specified time points. Mock samples were incubated with boiled caspase-3, and 0 h samples were removed at the start of each reaction. The 21mer dsRNA was loaded as size marker. (**d**) Lack of Dicer-1 catalytic activity in apoptotic cell extract. The enzymatically active cell extracts were prepared from the control or etoposide (VP16-70 μM for 18 h)-treated GM637 cells, which contained intact or partially cleaved hDicer-1 as determined by immunoblotting for Dicer-1 (left panel). The cell extracts were used in the *in vitro* Dicer activity assay for cell extracts. Aliquots of the assay mixture at various time points were resolved on non-denaturing 3.5–20% PAGE and stained with ethidium bromide. Size markers (lanes 1 and 2) were 27 and 21mer dsRNA that were spiked into the assay buffer without the cell extract. The results shown here represent similar results obtained with at least two independent experiments. (**e**) Depletion of miR-16, miR-21 and let-7a mature miRNA in the apoptotic HL-60 cells. The HL-60 cells were treated with etoposide for specified time, and small RNA extracted from the cells were loaded on 15% PAGE with 6 M Urea and northern-blotted. Membranes were probed with ^{32}P-labeled specific probes to examine the levels of three endogenous mature miRNAs (hsa-miR-16, hsa-miR-21 and hsa-let-7a). The staining of membrane with ethidium bromide (EtBr panel) was carried out to reflect equal loading (left panel). The signals from images of two analyses each from two independent experiments were quantified and shown here as mean ± S.D. values for relative miRNA expression as compared with untreated control cells (right panel)

nature of this observation irrespective of the fate or function of the target gene product during apoptosis. The fact that the transient RNAi achieved with 21mer siRNA was not affected during apoptosis indicated that RISC-dependent part of RNAi pathway does not fail during apoptosis. Our results can not exclude the possibility that RISC complex rapidly loaded with 21mer siRNA immediately after transfection could continue to function during apoptosis; however, our observation that Ago-2 remains intact during apoptosis supports the argument that RISC-dependent step of RNAi is not affected during apoptosis.

Using *in vitro* caspase assays, *in vivo* apoptotic cleavage of wild-type and mutant forms of tagged hDicer-1 and caspase-3-deficient MCF-7 cells, we show that Dicer-1 is specifically cleaved at two sites STTD^{1476} and the CGVD^{1538} within the RNase IIIa domain principally by caspase-3. A recent study has reported cleavage of Dicer-1 during apoptosis at the DHPD^{1644} site.[9] However, our results show that it is unlikely to be the main cleavage site of Dicer-1, because (a) cleavage at this site would result in a C-terminal fragment of $\sim$278 aa or $\sim$32 kDa, whereas we identified 42 or 50-kDa C-terminal fragments; (b) we show that D/A mutations at STTD^{1476} and CGVD^{1538} sites completely abolish Dicer-1 cleavage during apoptosis, whereas DHPD^{1644}/A mutation could not block Dicer-1 cleavage;[9] (c) the MS–MS analyses of C-terminal 42-kDa fragment revealed tryptic fragments starting at ^{1578}AAQL, which is $\sim$80-aa residues upstream of the DHPD^{1644} site. The earlier study also reported that Dicer-1 is cleaved by either caspases-3 or -7,[9] whereas we provide a reasonable proof using various approaches that cellular cleavage of Dicer-1 is consistent with its cleavage by caspase-3.

For many of the proteins cleaved at specific sites by caspases, the end result is either a strategic activation or inactivation of their function, which could either facilitate apoptosis or prevent the anti-apoptotic activity of the target protein.[8] Our study provides the first definitive proof of catalytic inactivation of Dicer-1 during apoptosis. We show that caspase-3-mediated cleavage of Dicer-1 *in vitro* reduces its catalytic activity, and that apoptotic cell extracts with cleaved ΔDicer-1 have a robust inhibition of catalytic dicing activity despite the presence of some intact Dicer-1. The latter suggests that additional events during apoptosis or presence of the cleaved fragments of Dicer-1 could contribute towards inactivation of catalytic activity of Dicer-1 during apoptosis (see below).

The cleavage of Dicer-1 at two distinct sites STTD^{1476} and CGVD^{1538} within RNase IIIa domain, allows us to propose a model for its catalytic inactivation during apoptosis. The structural studies with Giardia Dicer[25] and human Dicer or bacterial RNase III[26,27] suggest that RNase IIIa and IIIb domains of hDicer-1 form an intramolecular dimer, which, with the help of PAZ and dsRBD domains, cleave the long dsRNA substrate to the 21mer dsRNA. The catalytic center of Dicer is composed of two sets of identical motifs located in RNase IIIa and IIIb domains. These motifs with a conserved D or E residues are EXXX<u>D</u>^{1320} and DXX<u>E</u>^{1564} in RNase IIIa domain and EXXX<u>D</u>^{1709} and DXX<u>E</u>^{1813} in RNase IIIb domain. These four motifs allow Dicer to precisely touch the proximal or distal end of the cleavage sites on the long dsRNA substrate; hence, mutations at D or E residues in all four or even two of these motifs could abolish or significantly suppress catalytic function of Dicer-1.[27] Therefore, cleavage of Dicer-1 at D^{1476} and D^{1538} by caspase-3 would result in the separation of EXXXD^{1320} motif from the DXXE^{1564} motif within the RNase IIIa domain and inactivation of Dicer-1. Our results also suggest that neither the 180-kDa ΔDicer-1 containing one catalytic motif EXXXD^{1320} nor the 42-kDa C-terminal fragment containing the remaining three catalytic motifs can precisely carry out the catalytic function of full Dicer-1. In addition, it is possible that these two enzyme-dead fragments of Dicer-1 can cause *trans*-dominant inhibition of the residual intact Dicer-1 due to their potential to interact with the dsRNA substrates or other RNAi proteins including the RISC complex.

Finally, the cleavage and inactivation of Dicer-1 during apoptosis would have two major consequences (a) abrogation of DNA vector-based RNAi could influence results obtained with stable shRNA models that examine apoptosis and (b) reduced availability of mature miRNA may be of major consequence for miRNA-mediated control of apoptosis and cancer, as several miRNAs act as positive and negative regulators of cell death.[4]

Materials and Methods

Cells, DNA vector-based RNAi clones and apoptosis-inducing treatments and western blotting. Following cell lines were obtained from ATCC (unless specified otherwise) and grown in specified media obtained from GIBCO at 37°C in a humidified incubator with 5% CO_2, supplemented with 10% fetal bovine serum, 50 U/ml penicillin and 50 μg/ml streptomycin: human myeloid leukemic HL-60 (RPMI), human cervical carcinoma HeLa (DMEM-high glucose), monkey kidney COS-1 cells (DMEM-low glucose) and human breast adenoma MCF-7 cells (DMEM-low glucose).

Different stable RNAi clones were prepared as follows. The PARP-replete (U6) and PARP-depleted (SiP) cell lines derived from human skin fibroblasts (GM637, Coriell Cell Repository, MEM) and Chinese hamster ovary CHO cells (sub-line WT-5, α-MEM) were obtained as described earlier.[10] The human p14^{ARF}-expressing cell lines were created by stable transfection of CHO cells with HA-tagged p14^{ARF} cloned in pcDNA-3 expression vector (Invitrogen), followed by selection of geneticin (800 μg/ml)-resistant clones. One of the CHO-HA-ARF clones was subsequently transfected with a pBS-U6 vector containing human p14^{ARF}-targeting sequence 5′-GAAC ATG GTG CGC AGG TTC TT-3′ along with pTK-Hyg cDNA to isolate stable shARF clones, which were then maintained in medium containing geneticin (400 μg/ml) and hygromycin (200 μg/ml), as described earlier.[10,28] The DNA vector-based RNAi of lamin was achieved in HeLa cells after transfection with pBS-U6 vector containing lamin targeting sequence[29] and pTK-Hyg plasmid to isolate HeLa-shLamin clones that were maintained in medium containing 200 μg/ml hygromycin, as described earlier.[10]

Apoptosis was induced by treatment with one of the following reagents: 100 or 300 μM H_2O_2 (Sigma), 1 μM Staurosporin (Sigma), 1600 J/m^2 UVB (Spectrolinker XL-1000 UV cross-linker), 10 J/m^2 UVC, 10 or 100 μM MNNG (Sigma), 70 or 100 μM etoposide (VP-16) (Sigma), 1200 U/ml TNFα + 0.25 μg/ml actinomycin D (Sigma) and 1 or 5 μg/ml actinomycin D. For *in vivo* studies with a broad-spectrum caspase inhibitor, cells were pre-incubated with 50 μM of zVAD-fmk (Calbiochem) at 37°C for 90 min, followed by apoptosis-inducing treatment. Cells were harvested and extracts were analyzed by western blot.[10]

For the western blot, the extracts representing 200 000 cells or 20 μg protein were loaded on 6, 8, 12 or 6–15% SDS-PAGE, blotted on nitrocellulose, and probed with following antibodies: PARP (C-2-10, Aparptosis Inc., 1 : 10 000); 89-kDa PARP fragment (Abcam, 1 : 1000); human Dicer-1 (Abcam, 1 : 1000); human Ago-2 (Wako, 1 : 200); activated caspases-3 (Cell signaling, 1 : 1000); activated caspase-7 (Abcam, 1 : 200); FLAG (Sigma, 1 : 4000); HA (Sigma, 1 : 4000 or Covance 1 : 1000); actin (Sigma, 1 : 20 000) and GFP (BD Biosciences, 1 : 5000).

RNA isolation and RT-PCR. RNA was extracted with RNeasy mini kit (Qiagen). 250 ng of RNA was subjected to RT-PCR using the LightCycler RNA master SyBr green I kit in LightCycler Instrument (Roche) according to

manufacturer's protocol. The forward and reverse primers for PARP were 5′-AGTGACAGGCAAAGGCCAGGA-3′ (forward), 5′-CGCACCTGGCCCTTTTCTA TC-3′ (reverse). The primers of GAPDH were 5′-GAAGGTCGGAGTCAACGGAT TTGG-3′ (forward) and 5′-ACGGTGCCATGGAATTTGCCATGG-3′ (reverse). 10 μl of the PCR-amplified product was analyzed on 1.5% agarose gel containing ethidium bromide.

Transient knockdown with 21mer siRNA. All transient knockdown experiments were carried out in GM637 cells at 70% confluence in 60-mm dishes. For GFP expression and knockdown studies, a total of 5 μg of pGFP-N1 (Clontech) cDNA (or mock DNA: CMV plasmid) with or without 1 μg of 21mer GFP-targeting siRNA based on the sequence 5′-GCA AGC UGA CCC UGA AGU UCA U-3′ (Qiagen) were transfected by calcium phosphate protocol.[30] At 48 h after transfection, cells were treated with 100 μM etoposide for 18 h and cells were harvested for western blotting. For transient knockdown of PARP, GM637 cells were transfected with 600 pmol of 21mer siRNA (IDT) representing PARP-targeting sequence described for SiP912 vector[10] and 3 μg of pcDNA I/neo using lipofectamine 2000 (Invitrogen). Cells were maintained in 800 μg/ml geneticin for 96 h and treated with 100 μM etoposide (VP-16) for 24 h, followed by western blotting.

Wild-type and mutant hDicer-1: cloning, expression and immunopurification. The recombinant FLAG-hDicer-1 cDNA was created by in-frame cloning of the cDNA of hDicer-1 in the pCMV-3X-FLAG expression vector (Sigma) just after the 3X-FLAG tag at the 5′ end. The HA tag along with stop codon was inserted in the above cDNA at the 3′ end to create dual tagged FLAG-hDicer-1-HA cDNA. The caspase-uncleavable hDicer-1 D/A mutants were created from dual tagged hDicer-1 cDNA by site-directed mutagenesis (QuikChange-II-XL Site-directed mutagenesis kit, Stratagene). These cDNAs were transiently transfected in COS-1 cells (5–8 μg per 10-mm dish) with lipofectamine 2000 (Invitrogen). At 48 h after transfection, apoptosis-inducing treatments were carried out as specified for each figure, and cells either harvested for western blotting or subjected to immunopurification protocol using FLAG or HA-kits (Sigma).

At the end of the immunopurification protocol, the Dicer-1 or its fragments were processed in four different ways for different end uses. (i) For western blotting, beads were extracted with SDS-PAGE sample loading buffer and processed for western blotting. (ii) For the MS–MS analyses, the bead extracts were prepared as above for western blotting, resolved on 10% SDS-PAGE and stained with coomassie blue. The bands of interest, identified from a parallel western blot of the same samples, were excised from the gel and subjected to MS–MS analyses after tryptic digestion at the Taplin Biological Mass Spectrometry Services at the Harvard Medical School. (iii) For some of the *in vitro* caspase assays, FLAG-hDicer-1 was eluted from the beads by FLAG-peptide elution protocol (Sigma). (iv) For preparation of the bead-bound Dicer-1 for the *in vitro* caspase and dicing assays, the beads were washed and suspended at a concentration equivalent of Dicer-1-derived from 0.5×10^6 cells/μl of 50 mM Tris-Cl, pH 7.4 and 150 mM NaCl. The aliquots of bead-bound Dicer-1 were stored frozen at -80°C.

***In vitro* caspase cleavage assay.** For the *in vitro* cleavage assay with ten caspases, 50 ng of eluted FLAG-hDicer-1 was incubated with 1.5 U of recombinant-activated caspase (Biovision) in a 20-μl reaction mixture containing 20 mM PIPES, pH 7.2, 100 mM NaCl, 0.1% CHAPS, 1 mM EDTA, 10% sucrose, 10 mM DTT at 37°C for 90 min.[31] An aliquot was analyzed by the western blot for Dicer-1 and FLAG, as described above.

The *in vitro* caspase-3 cleavage assay using bead-bound FLAG-hDicer-1 was carried out in a total volume of 5 μl containing above stated caspase assay buffer,[31] 1.5 U of caspase-3 (Biovision) and 0.5–1 μl of immunobead-bound Dicer-1 that was pre-washed in the caspase assay buffer. The reaction was carried out at 37°C for up to 90 min with intermittent gentle vortexing to resuspend the beads. The reaction was terminated by addition of 5 μl of 2 $\times$ SDS-PAGE loading buffer and samples were heated at 95°C for 5 min, vortexed and eluted material was loaded on 6% SDS-PAGE, followed by transfer and western blotting for FLAG or Dicer-1, as described above.

***In vitro* Dicer-1 activity assays.** The catalytic dicing activity of Dicer-1 was measured in an assay derived from Kim *et al*.[19] that examined conversion of 27mer dsRNA substrate to 21mer dsRNA product. The 27mer dsRNA substrate was prepared based on the sequence used in the SiP912 vector for stable knockdown of PARP.[10] The sense oligo: 5′-CAA GCA CAG UGU CAA AGG UUU GGG C-3′ and the antisense oligo: 3′-CCG UUC GUG UCA CAG UUU CCA AAC CCG-5′, obtained from IDT were suspended at 100 μM in RNase-free duplex buffer (100 mM potassium acetate and 30 mM HEPES, pH 7.5), annealed at 94°C for 2 min, followed by gradual cooling at ambient temperature. The 100-μM 27mer dsRNA stocks were stored in aliquots at -30°C. The product 21mer dsRNA duplex was prepared based on PARP-targeting 21mer RNAi sequence[10] using the sense oligo: 5′-CAA GCA CAG UGU CAA AGG UUU-3′ and antisense oligo: 3′-CCG UUC GUG UCA CAG UUU CCA-5′, obtained from IDT and annealed exactly as above for 27mer dsRNA duplex.

For catalytic activity of Dicer-1 without pre-digestion with caspase-3, in a total reaction volume of 5 μl containing 20 mM Tris-Cl, pH 8.0, 200 mM NaCl, 2.5 mM $MgCl_2$ and 1 mM ATP, 25 pmol of 27mer dsRNA was digested with 0.5–1 μl immunobead-bound FLAG-hDicer-1, prepared as described above. The reaction was carried out at 37° for up to 16 h with intermittent gentle vortexing to resuspend the beads. The samples were mixed with 0.8 μl of 6 $\times$ DNA gel loading buffer (Fermentas), heated at 95°C for 5 min and electrophoresed on 20% native PAGE in 1 $\times$ TBE at 280 V for 70 min. The gel was stained in 0.5 μg/ml ethidium bromide for 30 min followed by two 5-min washes with water and visualized on ChemiGenius 2 (SynGene).

For the dicing activity assays after pre-digestion of Dicer-1 with caspase-3, the caspase-3 digestion *in vitro* was carried out for 90 min exactly as described above for immunobead-bound Dicer-1, and reagents were washed away by adding 100-μl dicer activity assay buffer (20 mM Tris-Cl, pH 8.0, 200 mM NaCl, 2.5 mM $MgCl_2$ and 1 mM ATP). The supernatant was discarded after centrifugation at 12 000 $\times$ *g* for 2 min, and the bead-bound digested Dicer-1 was suspended in 5 μl of dicing activity assay buffer to carry out the dicing reaction with 27mer dsRNA substrate, as described above.

For dicing activity assay using cell extracts, the enzymatically active cell extracts were prepared from control or apoptotic GM637cells, based on a modified protocol of Billy *et al*.[32] Briefly, cells were scraped in the medium, centrifuged at 500 $\times$ *g* for 5 min, washed twice with cold PBS and suspended in 50 mM Tris-Cl, pH 7.5 containing 150 mM NaCl, 2.5 mM $MgCl_2$, 5.5 mM DTT and EDTA-free protease inhibitor cocktail. Cells were lysed on ice by mild sonication using microtip probe for 2 $\times$ 15 s at 11 setting in Sonic Dismembranator (Fisher Scientific). The supernatant obtained after centrifugation at 16 000 $\times$ *g* for 5 min was supplemented with glycerol (10% v/v) and stored in aliquots at -30°C. The Dicer assay *in vitro* was carried out as described earlier. In brief, the cell extracts were adjusted to 1 mg protein/ml and 25 μl of extract was incubated with 125 pmol of 27mer dsRNA substrate at 37°C. At the end of the specified incubation period, 2.5-μl aliquots were resolved on 3.5–20% non-denaturing PAGE, and RNA was visualized by staining with 0.5 μg/ml ethidium bromide.[19]

miRNA extraction and northern blot. The total miRNA was extracted from HL-60 cells using the mirVana PARIS kit (Ambion) according to manufacturer's protocol. 2-μg small RNA was resolved on 15% PAGE in 6 M urea in 1 $\times$ Tris-borate-EDTA and transferred to charged nylon (Brightstar, Ambion). Two miRNA-specific DNA probes (Invitrogen) were based on sequences derived from http://microrna.sanger.ac.uk: Hsa-let-7a (5′-TGAGGTAGTAGGTTGTATAGTTTTT TCCTGTCTC-3′) and Hsa-miR-21 (5′-TAGCTTATCAGACTGATGTTGATTTTTT TTCCTGTCTC-3′). The RNA probe for Hsa-miR-16 (5′-GGGAGACAGGCGCC AAUAUUUACGUGCUGCUA-3′) was obtained from Ambion. The DNA and RNA probes were end-labeled with KinaseMax 5′-End-Labeling kit (Ambion). The northern blots of total miRNA were probed with ^{32}P-labelled probes prepared for each of the three miRNA according to manufacturer's instructions. The images were analyzed by Storm 860 with ImageQuant TL software (Amersham Pharmacia Biotech).

Acknowledgements. We are grateful to Véronique Richard for technical help. We are thankful to Martin Simard and Michele Rouleau of Laval University for helpful discussion and G Sui for shRNA constructs of ARF. We are thankful to Ross Tomaino of Taplin Biological Mass Spectrometry Facility at the Harvard Medical School for MS–MS analyses and interpretation of results. This work was supported by the research grants to GMS from Natural Sciences and Engineering Research Council of Canada (155257-06) and the National Cancer Institute of Canada with the funds from the Canadian Cancer Society (NCIC-16407). HHQ and FKK were supported by a CIHR-Post-Doctoral fellowship and an NSERC-Doctoral scholarship awards, respectively. EBA and GMS were

supported by an FRSQ-Junior-1 Scientist and FRSQ-Senior Scientist awards, respectively from the Fonds de la Recherche en Santé du Québec.

1. Filipowicz W, Jaskiewicz L, Kolb FA, Pillai RS. Post-transcriptional gene silencing by siRNAs and miRNAs. *Curr Opin Struct Biol* 2005; **15**: 331–341.
2. Shi Y. Mammalian RNAi for the masses. *Trends Genet* 2003; **19**: 9–12.
3. Jovanovic M, Hengartner MO. miRNAs and apoptosis: RNAs to die for. *Oncogene* 2006; **25**: 6176–6187.
4. Wiemer EA. The role of microRNAs in cancer: no small matter. *Eur J Cancer* 2007; **43**: 1529–1544.
5. Yuan J, Kramer A, Matthess Y, Yan R, Spankuch B, Gatje R *et al.* Stable gene silencing of cyclin B1 in tumor cells increases susceptibility to taxol and leads to growth arrest *in vivo*. *Oncogene* 2006; **25**: 1753–1762.
6. Gonzalez S, Perez-Perez MM, Hernando E, Serrano M, Cordon-Cardo C. p73beta-mediated apoptosis requires p57kip2 induction and IEX-1 inhibition. *Cancer Res* 2005; **65**: 2186–2192.
7. Zhang M, Zhou Y, Xie C, Zhou F, Chen Y, Han G *et al.* STAT6 specific shRNA inhibits proliferation and induces apoptosis in colon cancer HT-29 cells. *Cancer Lett* 2006; **243**: 38–46.
8. Fischer U, Janicke RU, Schulze-Osthoff K. Many cuts to ruin: a comprehensive update of caspase substrates. *Cell Death Differ* 2003; **10**: 76–100.
9. Matskevich AA, Moelling K. Stimuli-dependent cleavage of Dicer during apoptosis. *Biochem J* 2008; **412**: 527–534.
10. Shah RG, Ghodgaonkar MM, Affar EB, Shah GM. DNA vector-based RNAi approach for stable depletion of poly(ADP-ribose) polymerase-1. *Biochem Biophys Res Commun* 2005; **331**: 167–174.
11. Ghodgaonkar MM, Zacal NJ, Kassam SN, Rainbow AJ, Shah GM. Depletion of poly(ADP-ribose)polymerase-1 reduces host cell reactivation for UV-treated adenovirus in human dermal fibroblasts. *DNA Repair (Amst)* 2008; **7**: 617–632.
12. Nusinow DA, Hernandez-Munoz I, Fazzio TG, Shah GM, Kraus WL, Panning B. Poly (ADP-ribose) polymerase 1 is inhibited by a histone H2A variant, MACROH2A, and contributes to silencing of the inactive X chromosome. *J Biol Chem* 2007; **282**: 12851–12859.
13. Tentori L, Muzi A, Dorio AS, Bultrini S, Mazzon E, Lacal PM *et al.* Stable depletion of poly (ADP-ribose) polymerase-1 reduces *in vivo* melanoma growth and increases chemosensitivity. *Eur J Cancer* 2008; **44**: 1302–1314.
14. Zeini M, Traves PG, Lopez-Fontal R, Pantoja C, Matheu A, Serrano M *et al.* Specific contribution of p19(ARF) to nitric oxide-dependent apoptosis. *J Immunol* 2006; **177**: 3327–3336.
15. Ruchaud S, Korfali N, Villa P, Kottke TJ, Dingwall C, Kaufmann SH *et al.* Caspase-6 gene disruption reveals a requirement for lamin A cleavage in apoptotic chromatin condensation. *EMBO J* 2002; **21**: 1967–1977.
16. Cerutti H, Casas-Mollano JA. On the origin and functions of RNA-mediated silencing: from protists to man. *Curr Genet* 2006; **50**: 81–99.
17. Germain M, Affar EB, D'Amours D, Dixit VM, Salvesen GS, Poirier GG. Cleavage of automodified poly(ADP-ribose) polymerase during apoptosis. Evidence for involvement of caspase-7. *J Biol Chem* 1999; **274**: 28379–28384.
18. Janicke RU, Sprengart ML, Wati MR, Porter AG. Caspase-3 is required for DNA fragmentation and morphological changes associated with apoptosis. *J Biol Chem* 1998; **273**: 9357–9360.
19. Kim DH, Behlke MA, Rose SD, Chang MS, Choi S, Rossi JJ. Synthetic dsRNA Dicer substrates enhance RNAi potency and efficacy. *Nat Biotechnol* 2005; **23**: 222–226.
20. Cimmino A, Calin GA, Fabbri M, Iorio MV, Ferracin M, Shimizu M *et al.* miR-15 and miR-16 induce apoptosis by targeting BCL2. *Proc Natl Acad Sci USA* 2005; **102**: 13944–13949.
21. Chan JA, Krichevsky AM, Kosik KS. MicroRNA-21 is an antiapoptotic factor in human glioblastoma cells. *Cancer Res* 2005; **65**: 6029–6033.
22. Meng F, Henson R, Lang M, Wehbe H, Maheshwari S, Mendell JT *et al.* Involvement of human micro-RNA in growth and response to chemotherapy in human cholangiocarcinoma cell lines. *Gastroenterology* 2006; **130**: 2113–2129.
23. Johnson SM, Grosshans H, Shingara J, Byrom M, Jarvis R, Cheng A *et al.* RAS is regulated by the let-7 microRNA family. *Cell* 2005; **120**: 635–647.
24. Meng F, Henson R, Wehbe-Janek H, Smith H, Ueno Y, Patel T. The MicroRNA let-7a modulates interleukin-6-dependent STAT-3 survival signaling in malignant human cholangiocytes. *J Biol Chem* 2007; **282**: 8256–8264.
25. Macrae IJ, Zhou K, Li F, Repic A, Brooks AN, Cande WZ *et al.* Structural basis for double-stranded RNA processing by Dicer. *Science* 2006; **311**: 195–198.
26. Gan J, Tropea JE, Austin BP, Court DL, Waugh DS, Ji X. Structural insight into the mechanism of double-stranded RNA processing by ribonuclease III. *Cell* 2006; **124**: 355–366.
27. Zhang H, Kolb FA, Jaskiewicz L, Westhof E, Filipowicz W. Single processing center models for human Dicer and bacterial RNase III. *Cell* 2004; **118**: 57–68.
28. Sui G, Affar el B, Shi Y, Brignone C, Wall NR, Yin P *et al.* Yin Yang 1 is a negative regulator of p53. *Cell* 2004; **117**: 859–872.
29. Sui G, Soohoo C, Affar EB, Gay F, Shi Y, Forrester WC *et al.* A DNA vector-based RNAi technology to suppress gene expression in mammalian cells. *Proc Natl Acad Sci USA* 2002; **99**: 5515–5520.
30. Ausubel FM, Brent R, Kingston RE, Moore DD, Seidonan JG, Smith JA *et al. Introduction of DNA into Mammalian Cells* Ausubel FM, *et al.* (eds). John Wiley & Sons, New York, 1992.
31. Stennicke HR, Salvesen GS. Biochemical characteristics of caspases-3, -6, -7, and -8. *J Biol Chem* 1997; **272**: 25719–25723.
32. Billy E, Brondani V, Zhang H, Muller U, Filipowicz W. Specific interference with gene expression induced by long, double-stranded RNA in mouse embryonal teratocarcinoma cell lines. *Proc Natl Acad Sci USA* 2001; **98**: 14428–14433.

Supplementary Information accompanies the paper on Cell Death and Differentiation website (http://www.nature.com/cdd)